Engineering Geology 205 (2016) 12–23

Contents lists available at ScienceDirect

Engineering Geology

journal homepage: www.elsevier.com/locate/enggeo

A one-step Newmark displacement model for probabilistic seismic slope displacement hazard analysis

Wenqi Du [a,*], Gang Wang [b]

[a] Institute of Catastrophe Risk Management, Nanyang Technological University, 50 Nanyang Avenue, Singapore
[b] Dept. of Civil and Environmental Engineering, The Hong Kong University of Science and Technology, Clear Water Bay, Hong Kong

ARTICLE INFO

Article history:
Received 5 March 2015
Received in revised form 12 August 2015
Accepted 26 February 2016
Available online 2 March 2016

Keywords:
Earthquake-induced slope displacement
Newmark model
Probabilistic seismic slope displacement hazard analysis
One-step approach
Spatial correlation

ABSTRACT

Estimating the earthquake-induced sliding displacement is important in assessing the stability of slopes during earthquakes. Current Newmark displacement models generally use ground motion intensity measures (IMs) as predictors, and the uncertainties of predicting IM values need to be accounted for in probabilistic seismic slope displacement hazard analysis. This paper aims at developing a simple one-step predictive model for the Newmark displacement based on only four seismological parameters (moment magnitude, rupture distance, fault categories and shear wave velocity at top 30 m V_{s30}) rather than any IMs. The predictive model is suitable for critical acceleration from 0.02 g to 0.25 g, covering most of the susceptible earthquake-induced landslide cases. First, the proposed one-step model is compared with some recently developed IM-based Newmark displacement models. It is found that both the median predictions and the variabilities of the proposed one-step model are in reasonable agreement with those obtained by the IM-based models. Second, several hypothetical slopes are used to compare the slope displacement hazard curves between the one-step model and the IM-based models. The new model can be used as an alternative method for a fully probabilistic analysis of the earthquake-induced slope displacements. In addition, spatial correlations of the Newmark displacement residuals are also investigated using strong-motion data from the Northridge and Chi-Chi earthquakes.

1. Introduction

Estimating the seismic displacement of natural slopes is particularly important for risk assessment of earthquake-induced landslides. Newmark (1965) proposed a rigid sliding block model, which assumed that sliding is initialized when the shaking acceleration exceeds a critical acceleration, and the block continues to move along a shear surface until the relative velocity between the block and ground is zero. The critical acceleration (a_c) is determined by the properties of slopes (e.g., the strength of material, groundwater level and the geometric slope angle). The velocity-time history of the block is calculated by integrating the exceeded parts of acceleration with respect time; then the velocity-time history is integrated versus time to compute the sliding displacement for each sliding episode (Fig. 1). The cumulative sliding displacement is called Newmark displacement *D*. Although the Newmark model ignores the internal deformation of the sliding mass during shaking process, it is still applicable to natural slopes or landslides in stiff materials (Jibson, 2007). Jibson (2011) stated that the Newmark sliding-block analysis may provide the best estimation for the stability of slopes, compared with other types of analysis.

Since Newmark's pioneering work, many researchers have proposed predictive equations for the Newmark displacement using various ground motion database and functional forms in terms of a_c and ground-motion intensity measures (IMs), such as the peak ground acceleration (PGA) and Arias intensity (Ia) (Arias, 1970) (e.g., Ambraseys and Menu, 1988; Jibson, 2007; Saygili and Rathje, 2008; Hsieh and Lee, 2011; Urzúa and Christian, 2013). For example, Ambraseys and Menu (1988) proposed simple relationships to predict the Newmark displacement based on the acceleration ratio, which is defined as a_c over PGA, using 50 strong-motion records from eleven earthquakes. It is to be noted that all these predictive equations are regressed using the computed Newmark displacements rather than the observed slope displacement data.

Using the IM-based Newmark displacement model, the seismic slope displacement is estimated as a two-step approach: first, ground motion prediction equations (GMPEs) are used to estimate the median and variability of IMs; second, sliding displacement values can be predicted using the estimated IMs and a_c. In design practice, the sliding displacements are often estimated using ground-motion IMs at a specified hazard level, which can be readily obtained from ground-motion hazard maps based on probabilistic seismic hazard analysis (PSHA). Although it is simple, the probability of exceedance of the predicted displacement is actually unknown. Therefore, it is a pseudoprobabilistic approach. Since the variabilities in the IMs and the predicted displacements are not

* Corresponding author.
E-mail address: wqdu@ntu.edu.sg (W. Du).

http://dx.doi.org/10.1016/j.enggeo.2016.02.011
0013-7952/

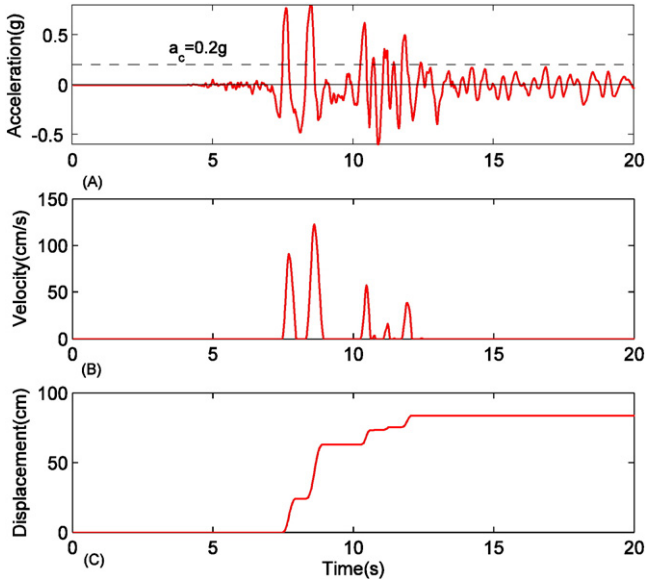

Fig. 1. Demonstration of computing Newmark displacement with critical acceleration $a_c = 0.2$ g: (A) Earthquake acceleration-time history, (B) Velocity of sliding block versus time and (C) Displacement of sliding block versus time.

quantified rigorously, the pseudoprobabilistic analysis usually results in non-conservative estimation in most cases compared with a fully probabilistic method (Rathje and Saygili, 2011).

To conduct a fully probabilistic seismic slope displacement hazard analysis (PSSDHA), the total variability of the computed displacement should be quantified, which is contributed from both GMPEs and the sliding displacement models. In addition, the epistemic uncertainty of GMPEs and the sliding displacement models should be taken into account. In a recent study, the epistemic uncertainty and aleatory variability in the two-step Newmark displacement analysis procedure have been systematically studied (Du and Wang, 2013a; Du and Wang, under review). The two-step approach would inevitably complicate the computational process, as two levels of integration process should be conducted to derive the probabilistic slope displacement hazard curves. This computational inefficiency will be much more remarkable if a large-scale region is studied (Du and Wang, 2014). In view of this, for the Newmark displacement, it may be not entirely necessary to use IMs as predictors, and, it is possible to estimate the sliding displacement directly based on seismological information and geological conditions rather than IMs. Then sliding displacement can be predicted directly by just one step instead of using the traditional two-step approach. The framework for conducting a fully probabilistic seismic slope displacement analysis using the proposed one-step model and the IM-based models, as well as the pseudoprobabilistic approach, are shown in Fig. 2.

This paper focuses on proposing a one-step empirical model to predict the Newmark displacement, directly based on seismological information and geological conditions rather than IMs. The model predictors are moment magnitude M_w, rupture distance R_{rup} (closest distance from the site to the ruptured area), shear wave velocity of the upper 30 m V_{s30}, and fault type. The Newmark displacement value can be regarded as a specific parameter that can be determined by seismological parameters associated with critical acceleration a_c. Furthermore, probabilistic seismic slope displacement hazard analyses for several hypothetic slopes are conducted by using the one-step model as well as the two-step IM-based models. The advantage of this one-step model is that it can greatly simplify this computational process in PSSDHA, meanwhile, the prediction results are generally similar with the existing two-step models. In addition, spatial correlations between the residuals of the proposed displacement model, which is required for analyzing spatially distributed slopes, are also studied. Two well recorded events, namely, the Chi-Chi and Northridge events, are used to compute the spatial correlations of displacement.

2. One-step Newmark displacement prediction model

2.1. Strong motion database

In this paper, the subset of the Pacific Earthquake Engineering Research Center's PEER-NGA strong motion database (Chiou et al., 2008) is used to compute the Newmark displacement. Only horizontal recordings from free-field conditions are used in the analysis, resulting in a total of 1560 pairs of ground motions of two horizontal directions from 64 worldwide earthquake events (Campbell and Bozorgnia, 2008). The selected records have moment magnitude in the range of 4.26 to 7.9, rupture distance from 0.07 km to 194 km and V_{s30} between 116.35 m/s and 2016 m/s. The distribution of these earthquake records with respect to magnitude and rupture distance, is shown in Fig. 3. For a given value a_c, the permanent displacement values can be obtained by aforementioned Newmark's sliding block method. Two horizontal recordings at the same station are treated as independent records. For each record, the maximum value computed from both the positive and negative directions for each record is taken as the permanent displacement.

2.2. The functional form

Regression analysis was performed to predict the sliding displacement as a function of seismological variables using mixed random effect algorithm proposed by Joyner and Boore (1993). The displacement prediction model takes a form as follows:

$$\ln(D_{ij}) = \overline{\ln(D_{ij})} + \eta_i + \varepsilon_{ij} \tag{1}$$

where $\ln(D_{ij})$ and $\overline{\ln(D_{ij})}$ represent the computed and the predicted logarithmic displacement value for the j-th recording and i-th event, respectively. η_i refers to inter-event residual (between earthquakes) and ε_{ij} denotes intra-event residual (within earthquakes), respectively. This model assumes that displacement values (D) follow logarithmic normal distribution. The mixed random effect model is widely applied to develop ground motion prediction equations, such as the NGA models (e.g., Campbell and Bozorgnia, 2008).

Since currently there is not any Newmark displacement model available in the literature using the mixed random effect regression, some functional forms that have been used for GMPEs are first attempted. More specifically, as the two commonly used predictors, PGA and Ia have been found to have a strong correlation with Newmark displacement (Wang, 2012). Therefore, the functional forms for predicting PGA and Ia could be used as the preliminary functional forms. After several trials and comparisons, the final functional expression is adopted as:

$$\ln(D) = c_1 + c_2 \cdot (8.5 - M_w)^2 + (c_3 + c_4 \cdot M_w) \ln\left(\sqrt{R_1^2 + h^2}\right) + c_5 \cdot Fr + (c_6 + c_7 \cdot M_w) \ln\left(\frac{R_{20}}{20}\right) + v_1 \cdot \ln\left(\frac{V_{s30}}{1100}\right) \tag{2}$$

where $R_1 = \begin{cases} R_{rup} & \text{if } R_{rup} \le 20km \\ 20 & \text{otherwise} \end{cases}$ and $R_{20} = \begin{cases} 20 & \text{if } R_{rup} \le 20km \\ R_{rup} & \text{otherwise} \end{cases}$; M_w refers to moment magnitude; R_{rup} means rupture distance (km); R_1 and R_{20} are two distance parameters: R_1 equals to R_{rup} when R_{rup} is smaller than 20 km, controlling the short-distance scaling. R_{20} changes if R_{rup} is greater than 20 km, controlling the long-distance scaling. Inclusion of R_1 and R_{20} in the functional form aims at better fitting empirical data in distance scaling. Fr is an indicator variable (1 for reverse and reverse-oblique types of faulting and 0 otherwise); h is a fictitious depth in km

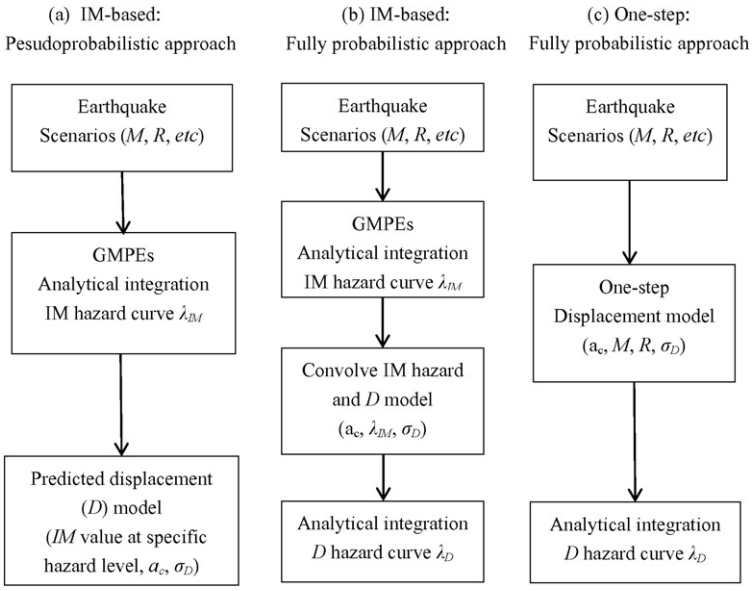

Fig. 2. Flow chart for psudoprobabilistic and fully probabilistic analysis of seismic slope displacement using the IM-based Newmark displacement model and the one-step model.

estimated during the regression, and V_{s30} represents the averaged shear wave velocity of the upper 30 m (m/s). The inclusion of fictitious depth h is to better fit the empirical data at short distances. The influence of site effects is incorporated in Eq. (2) by using the V_{s30} term. It is emphasized that the regression process is performed for different groups of critical accelerations a_c, due to the significant variations in various groups of a_c. This is unlike other IM-based displacement models that regress the empirical displacements for all a_c cases.

It is to be noted that Eq. (2) is regressed based only on sliding displacements larger than 0.01 cm. The probability of "zero" displacement ($D < 0.01$ cm) should also be predicted by seismological parameters. It is straightforward that the "zero" probability decreases as M_w increases, and increases as R_{rup} and V_{s30} increase. Using a probit regression analysis (Green, 2003), the probability of "zero" displacement ($D < 0.01$ cm) can be expressed as:

$$P(D=0) = 1-\Phi\left[c_8 + c_9 \cdot M_w + c_{10} \cdot \ln R_{rup} + c_{11} \cdot \ln(V_{s30})\right] \quad (3)$$

where Φ is the standard normal cumulative distribution function. The total displacement data (including smaller than 0.01 cm) are collected to derive Eq. (3). The model coefficients are estimated using the standard maximum likelihood procedure in *R* software. Therefore, the non-zero displacement values are estimated by Eq. (2), while Eq. (3) is used to specify the probability of zero displacement ($D < 0.01$ cm). Consequently, the predicted displacement according to a specified percentile p (in decimal form, i.e. $p = 0.5$ for the 50th percentile) can be determined as:

$$\ln D_p = \ln D + \sigma_D \cdot \Phi^{-1}\left(\frac{p - P(D=0)}{1 - P(D=0)}\right) \quad (4)$$

A total of thirteen coefficients are included in the one-step model. The regression process can be implemented in statistical programming using software like *R*, especially the 'nlme' function (Pinheiro et al., 2008). The regression coefficients for seven a_c values (0.02 g, 0.05 g, 0.075 g, 0.1 g, 0.15 g, 0.2 g and 0.25 g) are tabulated in Table 1. All coefficients yield small p-values, so they are statistically significant. For the cases that $a_c \geq 0.15$ g, c_4 and c_7 are statistically insignificant, so they

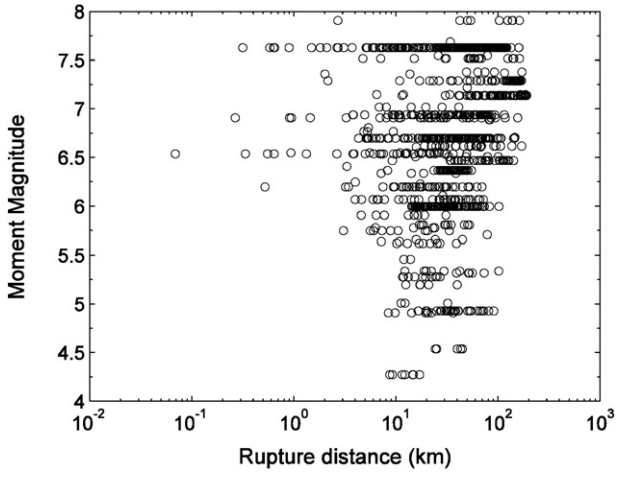

Fig. 3. Distribution of earthquake recordings with respect to moment magnitude and rupture distance.

Table 1
Coefficients of the proposed displacement model.

Coefficient	Critical acceleration (a_c)						
	0.02 g	0.05 g	0.075 g	0.1 g	0.15 g	0.2 g	0.25 g
c_1	8.15	8.23	7.11	7.29	7.13	6.12	15.21
c_2	−0.14	−0.18	−0.08	−0.14	−0.21	−0.25	−0.27
c_3	−5.04	−4.57	−5.17	−4.10	−2.77	−2.42	−5.33
c_4	0.45	0.31	0.40	0.22	–	–	–
c_5	0.54	0.64	0.75	0.72	0.80	0.74	1.04
c_6	−2.25	−4.84	−3.21	−4.67	−1.35	−1.65	−0.72
c_7	–	0.31	0.09	0.38	–	–	–
h	6.32	5.72	4.19	4.23	4.55	5.53	14.3
ν_1	−1.26	−1.26	−0.92	−0.86	−0.55	−0.57	−0.43
τ	0.45	0.39	0.50	0.54	0.45	0.42	0.29
σ	1.33	1.55	1.56	1.60	1.78	1.78	1.76
σ_t	1.40	1.59	1.63	1.70	1.84	1.82	1.78
c_8	1.04	3.69	4.52	4.13	4.10	2.76	1.53
c_9	1.46	0.97	0.76	0.64	0.37	0.28	0.26
c_{10}	−1.71	−1.74	−1.76	−1.78	−1.51	−1.27	−1.14
c_{11}	−0.37	−0.51	−0.52	−0.39	−0.37	−0.25	−0.15
No. of records used*	1168	934	715	562	381	270	192

Note: * denotes only records with PGA values larger than a_c can generate positive displacement values; τ: standard deviation of inter-event residuals; σ: standard deviation of intra-event residuals; σ_t: standard deviation of total residuals ($\sigma_t = \sqrt{\sigma^2 + \tau^2}$).

are removed in the final functional form. The reported inter- and intra-event standard deviations (in natural logarithmic scale) are also listed in this table. It is clear that the total standard deviation value generally increases as a_c increases, mainly due to the fewer available records used for larger a_c values. If a studied a_c value is not included in Table 1, it is suggested to interpolate the displacement in log space linearly between these obtained from neighboring a_c. Thus the one-step model is suitable for critical accelerations a_c ranging from 0.02 g to 0.25 g. For a case with $M_w = 7$, $R_{rup} = 10$ km, $V_{s30} = 600$ m/s and $a_c = 0.1$ g from a strike-slip fault, the estimated displacement by Eq. (2) is 4 cm, and the probability of "zero" displacement $P(D = 0)$ by Eq. (3) is 0.02. The median (50th percentile) estimated displacement can be calculated by Eq. (4) as 3.82 cm.

2.3. Inter-event and intra-event residuals

The distributions of inter- and intra-event residuals against predictors (M_w and R_{rup}) for $a_c = 0.05$ g and $a_c = 0.1$ g are shown in Fig. 4. The trend lines obtained by the simple linear regression are also plotted in these figures. No obvious biases between the residuals and the predictors can be found. The slightly biased trends in the intra-residuals versus the moment magnitude plots are possibly caused by a paucity of data at small magnitudes ($M_w < 5$). The distributions of the residuals imply that the proposed model can yield unbiased predicted displacement over a large magnitude and distance range.

The distribution of intra-event residuals against rupture distance shows a strong trend: the scatter of residuals generally increases with

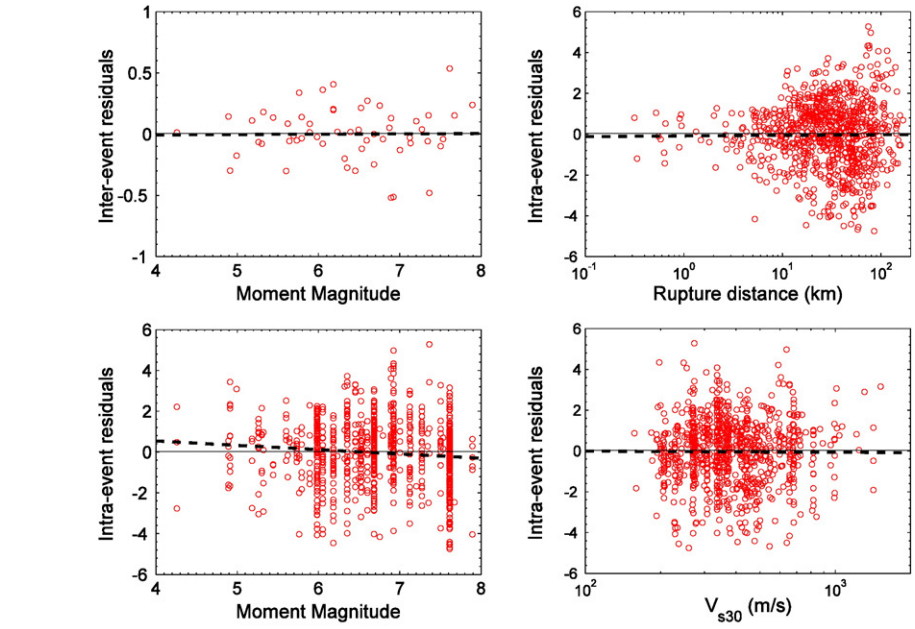

(a) a_c=0.05 g

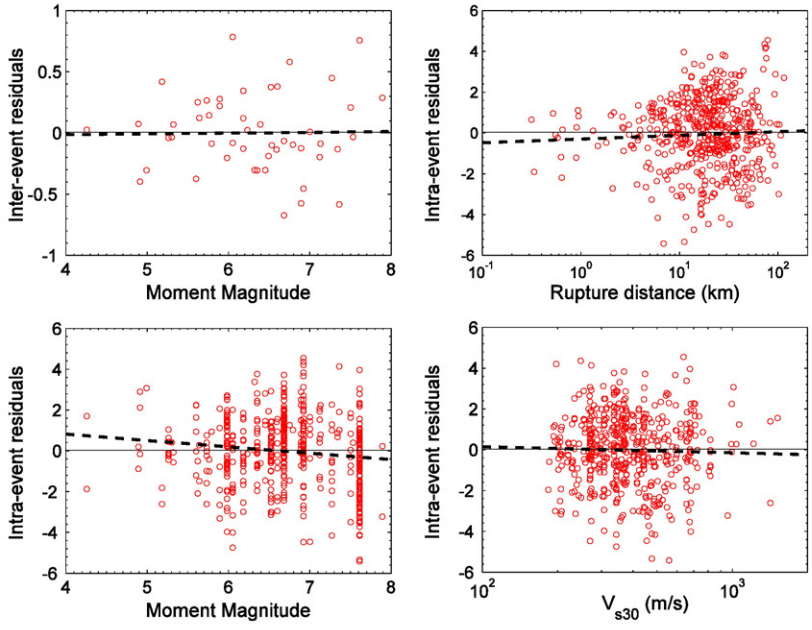

(b) a_c=0.1 g

Fig. 4. Distributions of inter-event and intra-event residuals with respect to moment magnitude, rupture distance and shear wave velocity for (a) $a_c = 0.05$ g and (b) $a_c = 0.1$ g, respectively.

increasing rupture distance. Hence, it is tempting to get the standard deviation of intra-event residuals within varying rupture distance bins, as shown in Fig. 5. The distance bins are partitioned into overlapping intervals in logarithmic scale from 0.1 km to 200 km, where the horizontal bar indicates the range of the interval in each bin. A simple trilinear model is used to represent the empirical data:

$$\sigma = \begin{cases} a & if \quad R_{rup} \le 1\ km \\ a + b \cdot \ln R_{rup} & if \quad 1\ km < R_{rup} < 100\ km \\ a + 4.6 \cdot b & if \quad 100\ km \le R_{rup} \le 200\ km \end{cases} \tag{5}$$

where a = 0.62, b = 0.21 for a_c = 0.02 g; a = 0.76, b = 0.23 for a_c = 0.05 g; a = 0.89, b = 0.237 for a_c = 0.075 g and a = 1.05, b = 0.22 for a_c = 0.1 g. For the case of $a_c \ge 0.15$ g, the rupture distance has little influence on the sigma value, so the reported constant values in Table 1 (e.g., σ = 1.78can be used for the case of a_c = 0.15 g) are recommended. For the standard deviation of the inter-event residuals, the constant values reported by regression analysis can be directly used since no obvious trend is observed.

3. Comparison with the IM-based displacement models

In this section, the proposed one-step model is compared with the IM-based Newmak displacement models in literature.

3.1. Median predicted values

Fig. 6 shows the predicted displacement of the proposed one-step model (Eq. (2)) with respect to rupture distance for various earthquake scenarios (generally large magnitude combined with small critical accelerations). The estimated displacement values from other Newmark displacement models are also shown for comparison. For simplicity purpose, one predictive model from each recent publication is selected in this study. These displacement models as well as their standard deviations are listed as follows:

1. [PGA] AM88 model (Ambraseys and Menu, 1988):

$$\log_{10}(D) = 0.9 + 2.53\log_{10}\left(\frac{a_c}{PGA}\right) - 1.09\log_{10}\left(\frac{a_c}{PGA}\right),\ \sigma_{\log_{10}D} = 0.3 \tag{6}$$

2. [PGA, M_w] BT07 model (Bray and Travasarou, 2007):

$$\ln(D) = -0.22 - 2.83\ln(a_c) - 0.333(\ln(a_c))^2 + 0.566\ln(a_c)\ln(PGA) + 3.04\ln(PGA) - 0.244(\ln(PGA))^2 + 0.278(M_w - 7)\ \sigma_{\ln D} = 0.66 \tag{7}$$

3. [PGA, Ia] J07 model (Jibson, 2007):

$$\log_{10}(D) = 0.561\log_{10}(Ia) - 3.833\log_{10}\left(\frac{a_c}{PGA}\right) - 1.474, \sigma_{\log_{10}D} = 0.616 \tag{8}$$

4. [PGA, Ia] RS08 model (Rathje and Saygili, 2008):

$$\ln(D) = 2.39 - 5.24\left(\frac{a_c}{PGA}\right) - 18.78\left(\frac{a_c}{PGA}\right)^2 + 42.01\left(\frac{a_c}{PGA}\right)^3 - 29.15\left(\frac{a_c}{PGA}\right)^4 - 1.56\ln(PGA) + 1.38\ln(Ia)\sigma_{\ln D} = 0.46 + 0.56(a_c/PGA) \tag{9}$$

5. [Ia] HL11 model (Hsieh and Lee, 2011):

$$\log_{10}(D) = 0.847\log_{10}(Ia) - 10.62a_c + 6.587a_c\log_{10}(Ia) + 1.84, \sigma_{\log_{10}D} = 0.295 \tag{10}$$

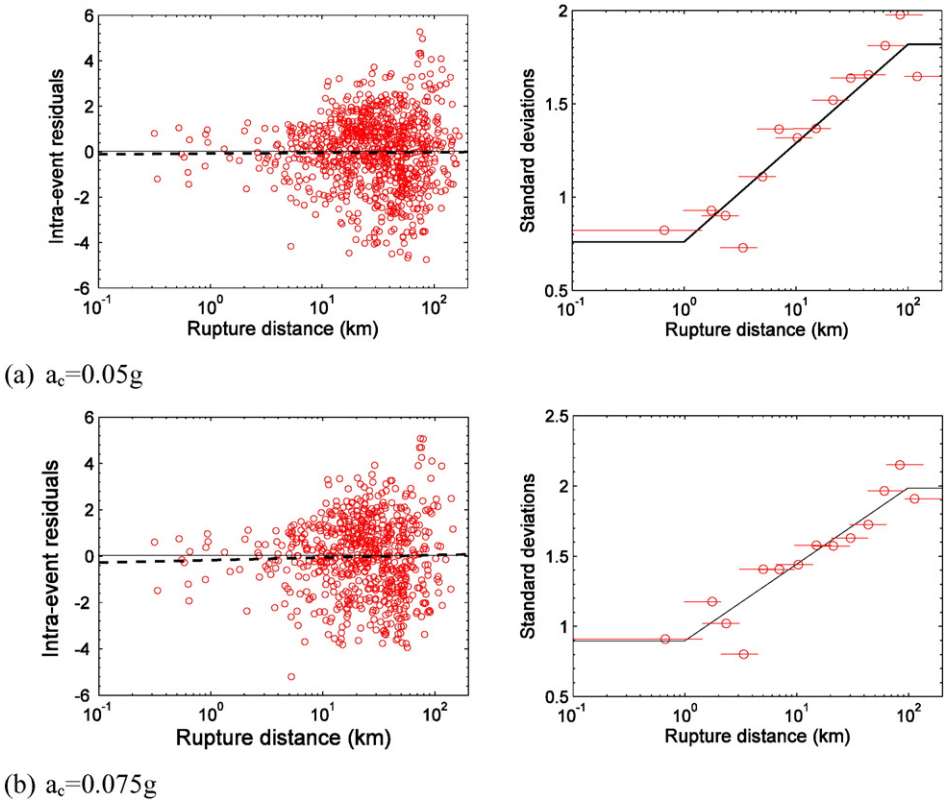

Fig. 5. Left: Distribution of intra-event residuals with respect to rupture distance; Right: trilinear relationship of intra-event standard deviations, where the point denotes the median value of each bin, and the horizontal bar indicates the range of the interval, respectively. Each range interval has at least 30 samples to get statistically reliable results.

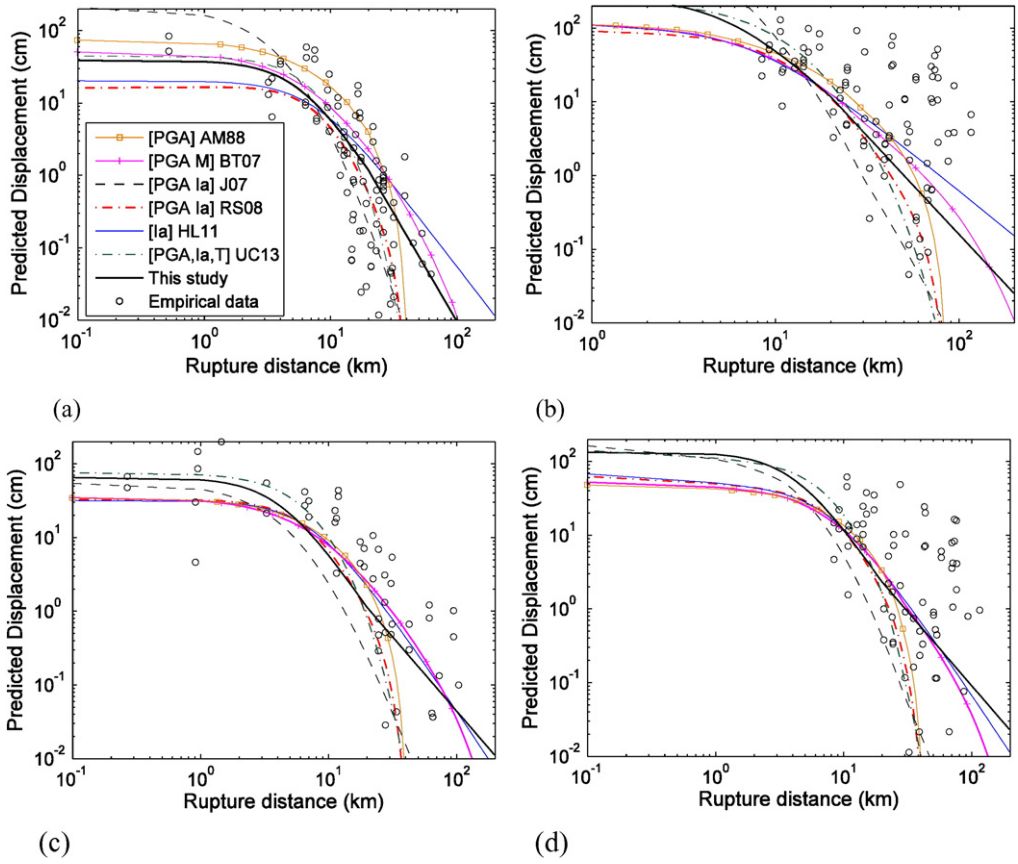

Fig. 6. Comparison of the one-step model (this study, Eq. (2)) with the other IM-based models (Eqs. (6)-(11)). The computed empirical displacement data using the NGA database are also shown for each scenario: (a) $M_w = 6$, strike-slip fault, $V_{s30} = 400$ m/s and critical accelerations $a_c = 0.05$ g; (b) $M_w = 7$, reverse fault, $V_{s30} = 400$ m/s and $a_c = 0.05$ g; (c) $M_w = 7$, strike-slip fault, $V_{s30} = 400$ m/s and $a_c = 0.1$ g and (d) $M_w = 7$, reverse fault, $V_{s30} = 400$ m/s and $a_c = 0.1$ g.

6. [PGA, Ia, T] UC13 model (Urzúa and Christian, 2013):

$$\log_{10}(D) = -0.1 - 4.3\left(\frac{a_c}{PGA}\right) + \log_{10}\left(\frac{Ia \cdot T}{PGA}\right) \quad (11)$$

In the above IM-based models, PGA, Ia, M_w and T are employed as predictors. For producing Fig. 6, the averaged PGA values from four NGA GMPE models (Abrahamson and Silva, 2008; Boore and Atkinson, 2008; Campbell and Bozorgnia, 2008; Chiou and Youngs, 2008) and the averaged Ia values from three predictive models (Travasarou et al., 2003; Foulser-Piggott and Stafford, 2012; Campbell and Bozorgnia, 2012) are regarded as input IMs for these IM-based models. In Eq. (11), T is predicted using the empirical equation of T_{avg} from Rathje et al. (2004). The empirical data computed from the selected NGA database are also shown in these plots. They are selected based on a combination of magnitude bin $[M_w - 0.25, M_w + 0.25]$ and shear wave velocity bin $[V_{s30} - 200$ m/s, $V_{s30} + 200$ m/s$]$. For example, Fig. 6(a) displays the empirical displacement data for $5.75 < M_w < 6.25$, $200 < V_{s30} < 600$ m/s, strike-slip fault and $a_c = 0.05$ g.

The comparison leads to the following observation: First, empirical data are almost evenly distributed around the predicted curves of the one-step model (this study), implying that this new model can get reasonably unbiased predictions for these earthquake scenarios. Second, the curves obtained by different models are generally comparable. Despite the difference in the functional forms and predictors that these equations are based on, quite consistent predictive values (especially for median rupture distance) can be seen from these plots. Large scatters can be observed in the far distance range, where the predicted displacements are very small with little engineering significance. Besides, although there are some discrepancies among these models, the predictive curves from the one-step model (this study) are generally located within the clusters of others. Hence, the new one-step model can reasonably predict the displacement values based directly on seismological variables.

The probability of zero displacement ($D < 0.01$ cm) is computed as a combination of the seismological parameters M_w, R_{rup} and V_{s30} (Eq. (3)). Fig. 7 shows the relationship between the predicted zero D probabilities, P(D = '0'), and these parameters and a_c. As expected, the probability of zero displacement increases significantly as a_c and R_{rup} increases, while it decreases if M_w increases.

The median predicted displacement of the new model can be calculated via Eqs. (2)-(4). Fig. 8 compares the median predicted sliding displacements by different models with respect to various a_c cases. For small a_c cases, all the models tend to predict similar displacement. For large a_c cases ($a_c > 0.2$ g), the new model and the BT07 models would result in generally smaller displacement predictions, mainly due to the probability of 'zero' (non-sliding) displacement considered during the regression. It is noted that the predicted displacements are generally small for large a_c cases and therefore they have little engineering significance.

3.2. Comparison of sigma values

As shown in Table 1, the total standard deviations of the one-step model are about 1.4–1.84 in the natural log scale for different a_c cases. It appears to be larger than any other reported sigma values of the IM-based models (Eqs. (6)-(11)), which range from 0.7 to 1.5 when

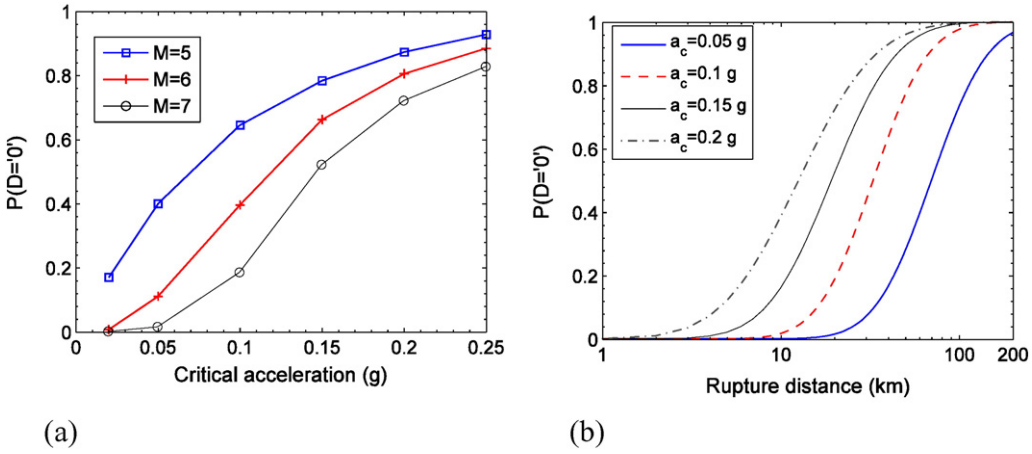

Fig. 7. (a) Predicted probability of "zero" displacement (Eq. (3)) versus a_c for earthquake scenarios: $R_{rup} = 20$ km, $V_{s30} = 400$ m/s; and (b) Predicted probability of "zero" displacement versus rupture distance for earthquake scenarios: $M_w = 7$ and $V_{s30} = 400$ m/s.

converted in the natural log scale. Yet, the total variability of the predicted Newmark displacements may still be comparable if the variabilities of the predictors, i.e., IMs, are also considered.

In this section, Monte-Carlo simulation is used to compute the total variability of the one-step and the two-step IM-based models for given earthquake scenarios. For the two-step models, vector IMs (e.g., PGA and Ia) can be reasonably assumed to follow multivariate normal distribution with median and standard deviation specified by GMPEs. The joint occurrence of multiple IMs is specified by using empirical correlations. The correlation coefficient between PGA and Ia is specified as $\rho(\text{PGA, Ia}) = 0.88$ (Campbell and Bozorgnia, 2012). First, 100 sets of correlated vector IMs are generated for a specific earthquake scenario. Second, for each set of vector IMs, 100 Newmark displacements can be simulated following a lognormal distribution with the median value and standard deviation specified by the predictive models (Eqs. (6)-(11)). The standard deviation of the resulted 10,000 displacement values is then calculated to estimate the total variability for each IM-based displacement model. For the one-step model, only 100 displacement residuals are required for each scenario.

Fig. 9 shows the standard deviations versus rupture distances for earthquake scenarios M_w 7.5 and M_w 6.5, respectively. For the IM-based models, the total sigma values considering both the variabilities of GMPEs and Newmark displacement models is about 1.5–2.5 for $a_c = 0.1$ g. By comparison, the sigma of the one-step displacement model reveals generally consistent curves. The new proposed model is not intended to reduce the total sigma values but to simplify the computational procedure.

4. Probabilistic seismic slope displacement hazard analysis (PSSDHA)

Traditional PSHA computed the ground motion hazard in terms of IM as:

$$\lambda_{IM}(z) = \lambda_0 \int_m \int_r P[IM>z|m,r] f(m) f(r) dm dr \quad (12)$$

where $\lambda_{IM}(z)$ refers to mean annual rate that IM (i.e., PGA) exceeds a given level z; λ_0 is the activity rate for this earthquake scenario; $f(m)$ and $f(r)$ represent probability density functions for earthquake magnitude (m) and source-to-site distance (r), respectively. $P[IM>z|m,r]$ is the conditional probability of IM exceeding z for a given m and r, which can be determined from a GMPE with the assumption that the IM follows a lognormal distribution. As is commonly used in practice (Abrahamson, 2000), the IM values are limited in the range of median value ± 3 standard deviations in integrating Eq. (12).

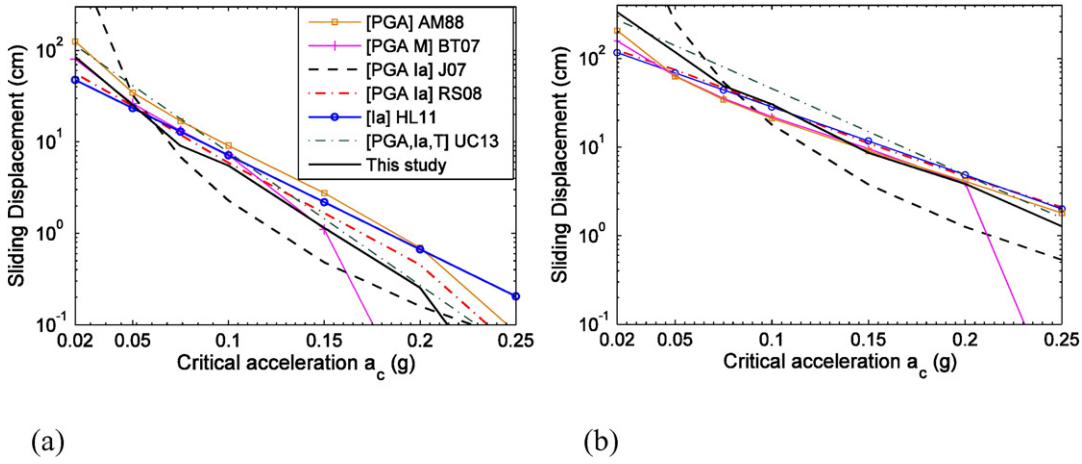

Fig. 8. Median predicted sliding displacement of various models against a_c values for earthquake scenario (a) $M_w = 7$, $R_{rup} = 10$ km, strike-slip fault, $V_{s30} = 400$ m/s and (b) $M_w = 7.5$, $R_{rup} = 5$ km, strike-slip fault, $V_{s30} = 400$ m/s. Note:$D_{0.5}$in Eq. (4) is used for the one-step model (this study). For the IM-based models, the averaged PGA from four NGA models and the averaged Ia values from three Ia models are used as input parameters.

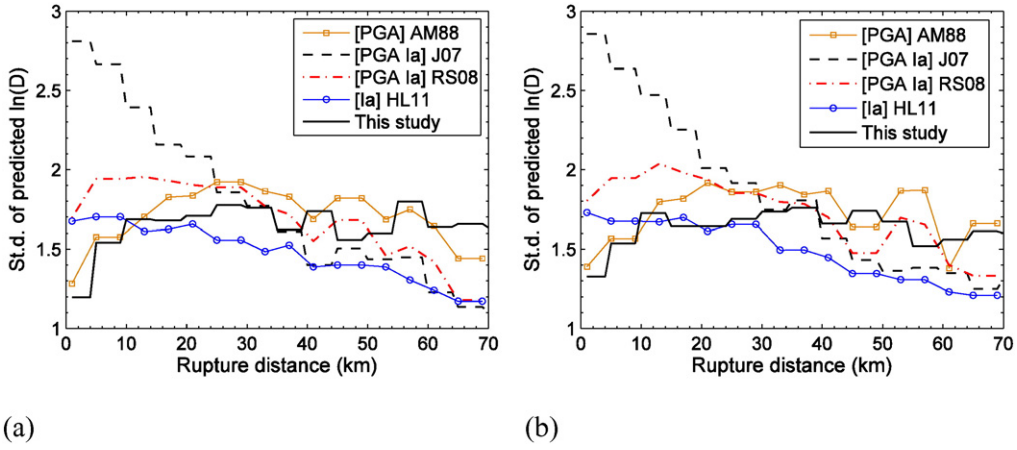

Fig. 9. Standard deviations considering the variability of GMPEs and Newmark displacement models, for $a_c = 0.1$ g and (a) M_w 7.5 (b) M_w 6.5, strike-slip fault, $V_{s30} = 400$ m/s earthquake scenarios. Cut-off displacement value is 0.01 cm. It is noted that small displacement values have to be excluded, since they are of little engineering importance but appear to be highly scattered in logarithmic scale.

Similar with λ_{IM}, the mean annual rate of exceedance$\lambda_D$for the sliding displacement value D can be represented as (Rathje and Saygili, 2008):

$$\lambda_D(x) = \int P[D \geq x | \mathrm{IM} = z] \cdot |d(\lambda_{\mathrm{IM}}(z))| \tag{13}$$

where $\lambda_D(x)$ is the mean annual rate that displacement exceeds a given value x; $P[D>x|IM=z]$ denotes the probability that the displacement value x is exceeded for a given IM value z (computed by scalar displacement equations e.g., Eq. (9)); and $|d(\lambda_{\mathrm{IM}}(z))|$ is the probability of occurrence for IM = z.

For the displacement models with two IMs as predictor variables (e.g., Eq. (8)), the joint probability density function for the vector IM must be considered (Bazzurro and Cornell, 2002). The analytical displacement hazard curve is calculated as:

$$\lambda_D(x) = \int P(D \geq x | \mathrm{IM}_1 = y, \mathrm{IM}_2 = z) f_{\mathrm{IM}_1,\mathrm{IM}_2}(y,z) dz dy \tag{14}$$

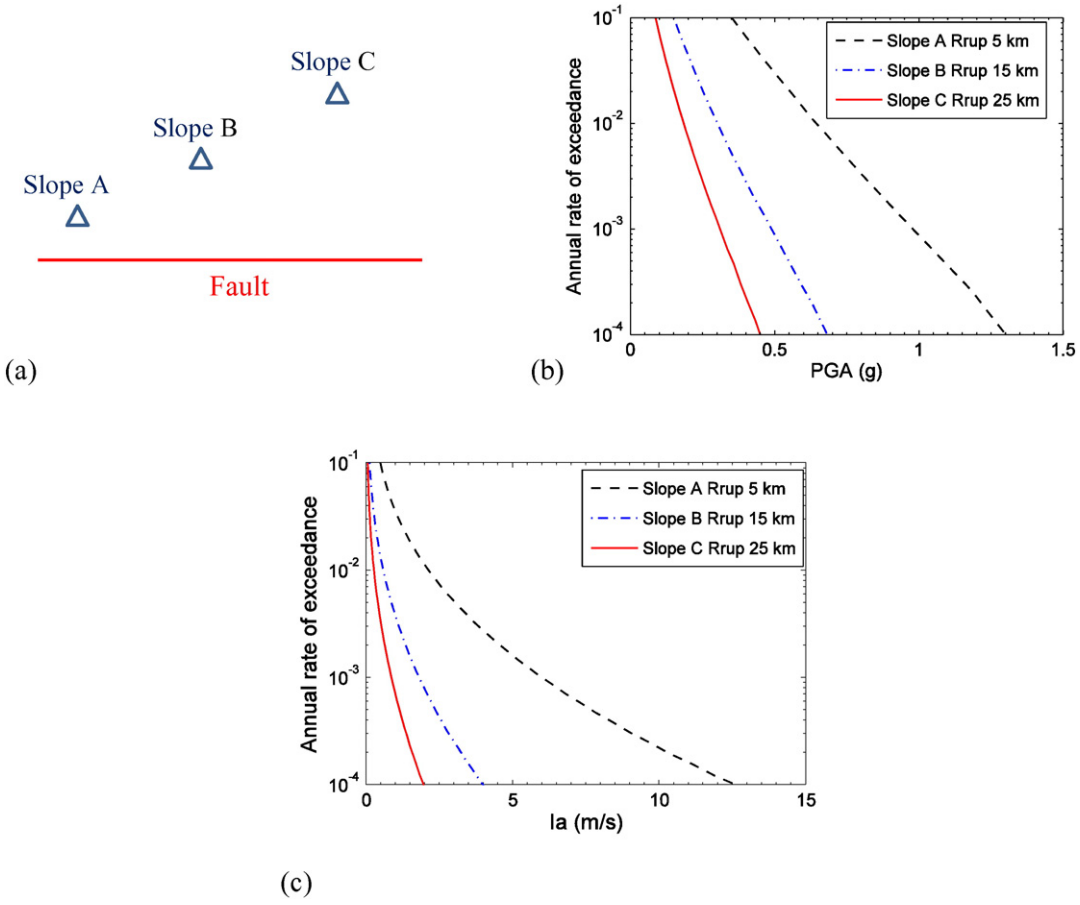

Fig. 10. (a) Locations of the three hypothetic slopes and the fault trace; (b) hazard curves for PGA; (c) hazard curves for Ia. For demonstration purpose, only predictive models proposed by Campbell and Bozorgnia (2008, 2012) are used to estimate the median and the variability of PGA and Ia, respectively.

where $f_{IM_1,IM_2}(y,z)$ denotes the joint occurrence probability for IM_1 equals y and IM_2 equals z, which can be given as:

$$f_{IM_1,IM_2}(y,z) = \lambda_0 \int_m \int_r f_{IM_1}(y|m,r) \cdot f_{IM_2|IM_1}(z|y,m,r) f(m) f(r) dmdr \tag{15}$$

where the term $f_{IM_1}(y|m,r)$ refers to probability density function for IM_1 conditional on m and r, and $f_{IM_2|IM_1}(z|y,m,r)$ is the probability density function for IM_2 conditional on m, r and IM_1 equals y. It is noted that the correlation coefficient ρ_{IM_1,IM_2} between IM_1 and IM_2 is required to obtain $f_{IM_1,IM_2}(y,z)$.

Eqs. (12)-(15) clearly illustrate the analytical displacement curves for the two-step models, which incorporates the GMPEs as well as the displacement models. For the vector IMs models, the correlation coefficients between two IMs are also necessary. On the other hand, for the one-step model, the corresponding displacement hazard is computed simply as:

$$\lambda_D(x) = \lambda_0 \int_m \int_r P[D>x|m,r] f(m) f(r) dmdr \tag{16}$$

where $P[D>x|m,r]$ is computed by the proposed displacement equations Eqs. (2)-(4). For Eq. (16), only displacement model is required to compute the displacement hazard curves.

4.1. An illustrative example

A hypothetical area is investigated to compare the different displacement models in PSSDHA. Three slopes (slope A, B and C in Fig. 10(a)) located on stiff soil conditions (V_{s30} = 400 m/s) are used to derive displacement hazard curves. The slopes A, B and C are assigned the following parameters: R_{rup} = 5 km, a_c = 0.2 g; R_{rup} = 15 km, a_c = 0.1 g; R_{rup} = 25 km, a_c = 0.05 g, respectively. The locations of the three slopes, as well as a 30 km-long linear strike-slip fault source, are shown in Fig. 10(a). The following Gutenberg–Richter relationship is assumed to describe the seismicity of the source:

$$\log_{10}\lambda_m = 4.4 - 1.0 M_w \tag{17}$$

where λ_m is the mean annual rate of exceedance for the moment magnitude M_w. A total of 32 earthquake scenarios ranging from 4.4 to 7.6 with a magnitude bin of 0.1 are generated for this fault. Note that choosing the above simple recurrence law is only for demonstration purpose. The location of rupture is randomly distributed along fault. The empirical equation from Wells and Coppersmith (1994) is used to estimate the fault rupture length for each scenario:

$$\log_{10}(L) = -3.22 + 0.69 M_w \tag{18}$$

where M_w is moment magnitude and L represents surface rupture length. As discussed previously, Eqs. (12)-(15) are used to derive the displacement hazard curves for the IM-based models. For the one-step

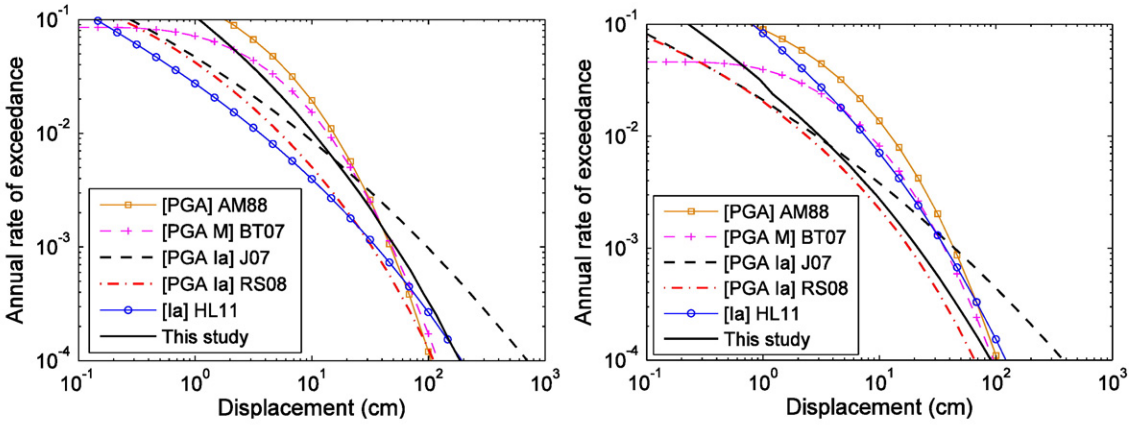

(a) Slope A (R_{rup} =5km; a_c =0.2 g) (b) Slope B (R_{rup} =15km; a_c =0.1 g)

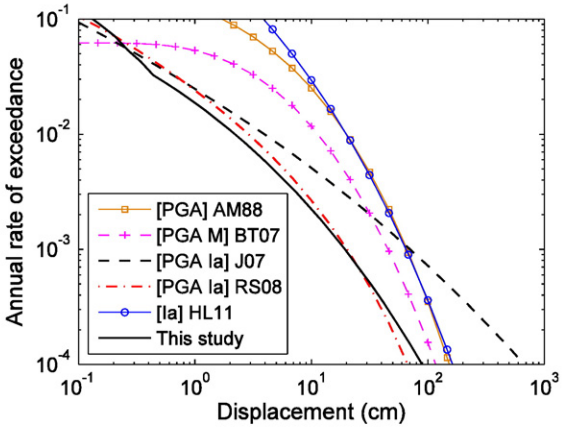

(c) Slope C (R_{rup} =25km; a_c =0.05 g)

Fig. 11. (a) (b) (c): Displacement hazard curves using different displacement models for Slopes A, B and C respectively. For IM-based models, only the predictive models proposed by Campbell and Bozorgnia (2008, 2012) are used in this example.

Table 2
Predicted Newmark displacement at specified hazard levels obtained from different displacement models.

Predicted Newmark displacement (cm)		Slope A		Slope B		Slope C	
Probability of exceedance in 50 years		10%	2%	10%	2%	10%	2%
Models	[PGA] AM88	36.4	67.5	31.2	65.1	48.4	97.0
	[PGA M_w] BT07	35.9	74.8	25.6	58.0	31.4	68.6
	[PGA Ia] J07	47.2	225.0	20.2	111.2	30.5	187.8
	[PGA Ia] RS08	20.3	58.8	10.7	32.3	12.5	35.9
	[Ia] HL11	19.1	76.0	24.2	63.4	46.2	97.5
	[M_w R_{rup} V_{s30}] This study	32.7	89.5	12.5	40.0	10.7	38.2

displacement model, Eq. (16) is the only equation needed to derive the displacement hazard curves.

For each slope, the 32 earthquake scenarios are considered to convolve IM hazard curves, which are necessary to derive displacement hazard curves for the IM-based models. Fig. 10 (b) and (c) show the hazard curves of PGA and Ia for the three slopes. For illustration purposes, only the predictive models proposed by Campbell and Bozorgnia (2008, 2012) are adopted to describe the median and the variability of PGA and Ia, respectively. Again, the IM values are limited in the range of median value ± 3 standard deviations in integration. Fig. 11 (a), (b) and (c) show the comparison of displacement hazard curves between the one-step model and the IM-based models for the slopes A, B and C, respectively. Integration in Eq. (16) is also limited within ± 3 standard deviations.

In general, the proposed one-step model can yield reasonably similar curves compared with the other models. If we select two hazard levels: 10% and 2% probability of exceedance in 50 years, the corresponding Newmark displacement obtained from different models are listed in Table 2. It is not our intention to judge which model is superior to the others or which model results in the most accurate prediction, but to provide an illustrative comparison between the one-step method and the two-step approaches. Since the one-step approach eliminates the necessity to predict the IMs, the computational process of the new model is much more efficient compared with the two-step models. This efficiency is much more predominant for complicated cases such as a regional-scale studied area. In addition, since selection of specific GMPEs would significantly affect the predicted displacement in the IM-based methods, the one-step approach can eliminate the epistemic uncertainties of predicting IMs.

5. Empirical spatial correlations of the displacement residuals

During an earthquake, the observed records show that the intra-event residuals of IMs are spatially correlated at nearby sites, due to the same source, similar wave propagation and similar geological conditions. Some researchers have quantified the spatial correlations of IMs as functions of separation distance (e.g., Boore et al., 2003; Jayaram and Baker, 2009; Du and Wang, 2013b), as well as the spatial correlations of building response parameters (e.g., DeBock et al., 2014). These spatial correlation models are indispensable to estimate seismic losses accurately for spatially distributed structures and infrastructures. Similarly, this section focuses on studying the spatial correlations of the displacement residuals.

Semivariograms are frequently used to quantify the spatial correlation of a random field (Goovaerts, 1997). Under the assumptions that the displacement field is isotropic and second-order stationary, the empirical semivariogarms of intra-event residuals of displacement can be computed as:

$$\tilde{\gamma}(h) = \frac{1}{2|N(h)|}\sum_{i=1}^{N(h)}\left[z_{u_i+h} - z_{u_i}\right]^2 \tag{19}$$

where $\tilde{\gamma}$ represents empirical semivariogram; $N(h)$ is the number of data pairs within this distance bin h, and z_{u_i+h} and z_{u_i} represents the ith data pair of intra-event residuals with separation distance h. An exponential function is usually adopted to fit the empirical semivariograms:

$$\gamma(h) = a(1 - \exp(-3h/b)) \tag{20}$$

where h refers to separation distance (km), and a and b are the sill and the range of semivariograms, respectively. The spatial correlation relation can be simplified as (please see more details in Goovaerts, 1997):

$$\rho_\varepsilon(h) = \exp(-3h/b) \tag{21}$$

where $\rho_\varepsilon(h)$ denotes the estimated correlation coefficient between the intra-event residuals with a separation distance h. It can be seen that once the correlation range b is obtained, the spatial correlation against any separation distance h can be fully quantified. Clearly this correlation ρ equals 1 at zero separation distance and decreases to zero if h increases to infinity.

The intra-event displacement residuals of the Chi-Chi and Northridge earthquakes are used in this paper. This is because only these two earthquakes in current dataset can provide sufficient data, especially in small separation distance bins. The detailed information for the two earthquakes is shown in Table 3. Fig. 12 displays the distribution of empirical data for the case of $a_c = 0.1$ g. The computed ranges of displacement residuals are 16 km and 8 km for the Chi-Chi and Northridge events, respectively. By contrast, the previously estimated spatial ranges of the PGA and Ia for these two earthquakes are shown in Table 3. Similar ranges can be found for the Northridge earthquake, while for the Chi-Chi event, the correlation range of the Newmark displacement D is significantly smaller than that of IMs. This is possibly due to the fact that the sliding displacement represents highly nonlinear structural response. Therefore, their spatial correlations are limited in range compared to the range of the IMs. In addition, the available records for estimating the correlation of displacement residuals are much fewer than the records used to estimate the correlation of IMs. Since currently only two events are available in the database, and the spatial correlations of displacement are dependent on specific a_c values, it is not feasible to propose a generalized spatial correlation model for Newmark displacement.

6. Discussions

Newmark displacements are commonly taken as a measure of regional-scale seismic landslide hazard estimation (e.g., Jibson et al.,

Table 3
Detailed information and computed ranges for the Chi-Chi and Northridge earthquakes.

Earthquake name	Date (dd/mm/yyyy)	Moment magnitude	Fault mechanism	Computed spatial correlation range[a] (km)		
				Newmark D ($a_c = 0.1$ g)	PGA	Ia
Chi-Chi	09/20/1999	7.62	Reverse-oblique	16	42.5	37.5
Northridge	01/17/1994	6.69	Reverse	8	7.6	7.9

[a] The computed spatial correlation ranges for PGA and Ia are obtained by Du and Wang (2013b).

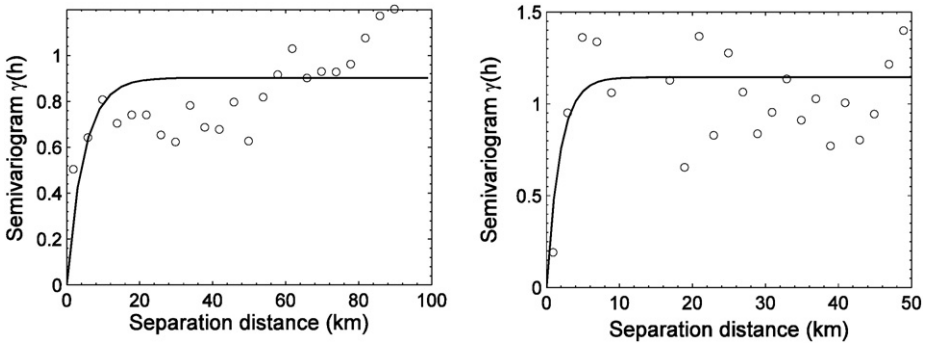

Fig. 12. The empirical semi-variograms and fitted exponential curves for the intra-event residuals of displacements for (a) the Chi-Chi earthquake and (b) the Northridge earthquake. The predicted Newmark displacement is calculated assuming $a_c = 0.1$ g.

2000; Jibson and Michael, 2009; Saygili and Rathje, 2009). The distribution of computed Newmark displacements is often used to identify potential landslide zones. Since it is particularly important to assess the seismic hazard of infrastructures or lifelines, the large-scale estimation of seismic landslide susceptibility should be studied as top priority (Wasowski et al., 2011). To conduct a probabilistic seismic slope displacement hazard analysis (PSSDHA) in a large scale, the uncertainties in the GMPEs and in the displacement models should be well incorporated over the whole region. This would inevitably bring in significantly computational cost. The purpose of this paper is to try to simplify the computational process: the Newmark displacement can be estimated directly by seismological information as well as geological conditions. Therefore, the proposed one-step displacement model is particularly suitable for PSSDHA in regional-scale cases. It is noted that earthquake-induced rock-falls in steep mountains are not considered in the present study. They are mainly triggered by high levels of ground shaking due to topographic amplification (e.g., Sepúlveda et al., 2005).

The proposed model includes thirteen coefficients changing with critical accelerations. Although it seems complicated, the model is still convenient to use once the input parameters and critical accelerations are obtained. For any a_c values in the range of 0.02 g to 0.25 g, the sliding displacement can be linearly interpolated in log space between neighboring a_c in Table 1. As mentioned previously, since using the simplified pseudoprobabilistic approach would yield inaccurate estimation, the proposed one-step method is indeed a simplification for fully probabilistic displacement analysis. This paper intends to provide an alternative displacement model, rather than reducing the use of IM-based models. Both the one-step model and IM-based models can be used for practical cases, and engineers can choose the most appropriate model depending on specific engineering applications.

One major challenge to improve the evaluation of seismic slope stability is to obtain accurate critical acceleration maps across the region. Some scholars (e.g., Dreyfus et al., 2013) have pointed out that the estimation of shear strength played a vital role in predicting the sliding displacement, and, generally overly conservative (low) shear-strength values would result in an over-estimation of landslide susceptibility. On the other hand, failure depth, material strength and groundwater data may vary significantly over a large region. Due to this challenge, more attention should be paid to a reliable estimation of the spatial distribution of a_c values in the future.

7. Conclusions

This paper provides a new one-step Newmark displacement model for critical acceleration within 0.02 g–0.25 g. Unlike most current Newmark displacement models using IMs as parameters, the proposed model gives an estimation of the sliding displacement directly based on seismological information and site conditions (i.e., M_w, R_{rup}, V_{s30} and fault category). Compared to the IM-based displacement models, the new model can result in reasonably consistent estimation of displacement for various cases. Therefore, it can be used as an alternative model to estimate the Newmark displacement.

The intra-event residuals of the one-step model clearly reveal significant trends with respect to rupture distance. A heteroskedastic intra-event standard deviation structure is adopted in this model, which can better predict the variance components than a homoscedastic model. The estimated total standard deviations are in the range of 0.6 to 2.1 in natural log scale, depending on the a_c values as well as rupture distances. Although it appears to be much larger than any IM-based models, this total variability of the Newmark displacement obtained from the one-step method is actually comparable with that obtained from IM-based models, if the variabilities of both the Newmark displacement predictions and IMs are incorporated in the two-step procedure.

Application of the one-step model in probabilistic seismic slope displacement hazard analysis (PSSDHA) is also demonstrated using several hypothetic slopes. It is observed that the one-step model can result in displacement hazard curves comparable with the two-step models. Yet, the one-step model can greatly simplify the analytical procedure and computational cost, and is more suitable for large scale applications.

The spatial correlations for the residuals of the Newmark displacement are also investigated using two earthquake events. As a general recommendation, the correlation ranges obtained from the Northridge and Chi-Chi events, namely, 8 km and 16 km, are suggested to represent the spatial correlations of displacement residuals for heterogeneous and homogeneous fields, respectively.

Acknowledgments

The work described in this paper was supported by Hong Kong Research Grants Council through Collaborative Research Fund grant No. CityU8/CRF/13G and General Research Fund grant No. 16213615. The authors thank two anonymous reviewers for their helpful comments to improve this manuscript.

References

Abrahamson, N.A., 2000. State of the practice of seismic hazard evaluation. Proc. GeoEng 2000, Melbourne, Australia vol. 1, pp. 659–685.
Abrahamson, N.A., Silva, W.J., 2008. Summary of the Abrahamson & Silva NGA ground-motion relations. Earthquake Spectra 24 (1), 67–97.
Ambraseys, N.N., Menu, J.M., 1988. Earthquake-induced ground displacements. Earthq. Eng. Struct. Dyn. 16 (7), 985–1006.
Arias, A., 1970. Measure of earthquake intensity. In: Hansen, R.J. (Ed.), Seismic design for nuclear power plants. Massachusetts institute of technology press, Cambrige, MA, pp. 438–483.
Bazzurro, P., Cornell, C.A., 2002. Vector-Valued Probabilistic Seismic Hazard Analysis (VPSHA). Seventh U.S. National Conference on Earthquake Engineering vol. II. EERI, pp. 1313–1322.
Boore, D.M., Atkinson, G.M., 2008. Ground-motion prediction equations for the average horizontal component of PGA, PGV and 5%-damped PSA at spectral periods between 0.01 s and 10s. Earthquake Spectra 24 (1), 99–138.
Boore, D.M., Gibbs, J.F., Joyner, W.B., Tinsley, J.C., Ponti, D.J., 2003. Estimated ground motion from the 1994 Northridge, California, earthquakes at the site of the interstate

10 and La Cienega Boulevard bridge collapse, West Los Angeles, California. Bull. Seismol. Soc. Am. 93 (6), 2737–2751.
Bray, J.D., Travasarou, T., 2007. Simplified procedure for estimating earthquake-induced deviatoric slope displacements. J. Geotech. Geoenviron. 133, 381–392.
Campbell, K.W., Bozorgnia, Y., 2008. NGA ground motion model for the geometric mean horizontal component of PGA, PGV, PGD and 5% damped linear elastic response spectra for periods ranging from 0.1 to 10 s. Earthquake Spectra 24 (1), 139–171.
Campbell, K.W., Bozorgnia, Y., 2012. A comparison of ground motion prediction equations for Arias intensity and cumulative absolute velocity developed using a consistent database and functional form. Earthquake Spectra 28 (3), 931–941.
Chiou, B., Youngs, R.R., 2008. An NGA model for the average horizontal component of peak ground motion and response spectra. Earthquake Spectra 24 (1), 173–215.
Chiou, B., Darragh, R., Gregor, N., Silva, W., 2008. NGA project strong motion database. Earthquake Spectra 24 (1), 23–44.
DeBock, D.J., Garrison, J.W., Kim, K.Y., Liel, A.B., 2014. Incorporation of spatial correlations between building response parameters in regional seismic loss assessment. Bull. Seismol. Soc. Am. 104 (1), 214–228.
Dreyfus, D., Rathje, E.M., Jibson, R.W., 2013. The influence of different simplified sliding-block models and input parameters on regional predictions of seismic landslides triggered by the Northridge earthquake. Eng. Geol. 163, 41–54.
Du, W., Wang, G., 2013a. Quantifying epistemic uncertainty and aleatory variablity of Newmark displacements under scenario earthquakes. 4th International Symposium on Geotechnical Safety and Risk, Hong Kong, December 4-6, 2013.
Du, W., Wang, G., 2013b. Intra-event spatial correlations for cumulative absolute velocity, Arias intensity and spectral accelerations based on regional site conditions. Bull. Seismol. Soc. Am. 103 (2 A), 1117–1129.
Du, W., Wang, G., 2014. Fully probabilistic seismic displacement analysis of spatially distributed slopes using spatially correlated vector intensity measures. Earthq. Eng. Struct. Dyn. 43 (5), 661–679.
Du, W., Wang, G., 2015. Quantification of epistemic uncertainty and aleatory variability in Newmark displacement analysis Submitted to Soil Dyn. Earthq. Eng. (under review).
Foulser-Piggott, R., Stafford, P.J., 2012. A predictive model for Arias intensity at multiple sites and consideration of spatial correlations. Earthq. Eng. Struct. Dyn. 41 (3), 431–451.
Goovaerts, P., 1997. Geostatistics for Natural Resources Evaluation. Oxford University Press, Oxford, New York.
Green, W., 2003. Econometric Analysis. fifth ed. Prentice Hall.
Hsieh, S.Y., Lee, C.T., 2011. Empirical estimation of Newmark displacement from the Arias intensity and critical acceleration. Eng. Geol. 122, 34–42.
Jayaram, N., Baker, J.W., 2009. Correlation model for spatially distributed ground-motion intensities. Earthq. Eng. Struct. Dyn. 38, 1687–1708.
Jibson, R.W., 2007. Regression models for estimating coseismic landslide displacement. Eng. Geol. 91, 209–218.
Jibson, R.W., 2011. Methods for assessing the stability of slopes during earthquakes—A retrospective. Eng. Geol. 122 (1), 43–50.
Jibson, R.W., Michael, J.A., 2009. Maps showing seismic landslide hazards in Anchorage, Alaska. U.S. Geological Survey Scientific Investigations Map 3077 (11 pp.).
Jibson, R.W., Harp, E.L., Michael, J.A., 2000. A method for producing digital probabilistic seismic landslide hazard maps. Eng. Geol. 58 (3), 271–289.
Joyner, W.B., Boore, D.M., 1993. Methods for regression analysis of strong-motion data. Bull. Seismol. Soc. Am. 83, 469–487.
Newmark, N.M., 1965. Effects of earthquakes on dams and embankments. Géotechnique 15 (2), 139–160.
Pinheiro, J., Bates, D., DebRoy, S., Sarkar, D., R Core team, 2008. NLME: linear and nonlinear mixed effects models (R package version; 3) pp. 1–89.
Rathje, E.M., Saygili, G., 2008. Probabilistic seismic hazard analysis for the sliding displacement of slopes: scalar and vector approaches. J. Geotech. Geoenviron. 134 (6), 804–814.
Rathje, E.M., Saygili, G., 2011. Estimating fully probabilistic seismic sliding displacements of slopes from a pseudoprobabilistic approach. J. Geotech. Geoenviron. 137 (3), 208–217.
Rathje, E.M., Faraj, F., Russell, S., Bray, J.D., 2004. Empirical relationships for frequency content parameters of earthquake ground motions. Earthquake Spectra 20 (1), 119–144.
Saygili, G., Rathje, E.M., 2008. Empirical predictive models for earthquake-induced sliding displacements of slopes. J. Geotech. Geoenviron. 134 (6), 790–803.
Saygili, G., Rathje, E.M., 2009. Probabilistically based seismic landslide hazard maps: an application in Southern California. Eng. Geol. 109, 183–194.
Sepúlveda, S.A., Murphy, W., Jibson, R.W., Petley, D.N., 2005. Seismically induced rock slope failures resulting from topographic amplification of strong ground motions: the case of Pacoima Canyon, California. Eng. Geol. 80 (3), 336–348.
Travasarou, T., Bray, J.D., Abrahamson, N.A., 2003. Empirical attenuation relationship for arias intensity. Earthq. Eng. Struct. Dyn. 32, 1133–1155.
Urzúa, A., Christian, J.T., 2013. Sliding displacements due to subduction-zone earthquakes. Eng. Geol. 166, 237–244.
Wang, G., 2012. Efficiency of scalar and vector intensity measures for seismic slope displacements. Front. Struct. Civ. Eng. 6 (1), 44–52.
Wasowski, J., Keefer, D.K., Lee, C.T., 2011. Toward the next generation of research on earthquake-induced landslides: current issues and future challenges. Eng. Geol. 122 (1), 1–8.
Wells, D.L., Coppersmith, K.J., 1994. New empirical relationships among magnitude, rupture length, rupture width, rupture area, and surface displacement. Bull. Seismol. Soc. Am. 84 (4), 974–1002.